RSC Advances

This is an *Accepted Manuscript*, which has been through the Royal Society of Chemistry peer review process and has been accepted for publication.

*Accepted Manuscripts* are published online shortly after acceptance, before technical editing, formatting and proof reading. Using this free service, authors can make their results available to the community, in citable form, before we publish the edited article. This *Accepted Manuscript* will be replaced by the edited, formatted and paginated article as soon as this is available.

You can find more information about *Accepted Manuscripts* in the Information for Authors.

Please note that technical editing may introduce minor changes to the text and/or graphics, which may alter content. The journal's standard Terms & Conditions and the Ethical guidelines still apply. In no event shall the Royal Society of Chemistry be held responsible for any errors or omissions in this *Accepted Manuscript* or any consequences arising from the use of any information it contains.

ROYAL SOCIETY OF CHEMISTRY

www.rsc.org/advances

# Temperature stress on thin film transistor with novel BaZnSnO semiconductor using solution process

**Jun Li [a,b*], Chuan-Xin Huang [a], Jian-Hua Zhang [b*], Wen-Qing Zhu [a], Xue-Yin Jiang [a], Zhi-Lin Zhang [a, b]**

[a] School of Material Science and Engineering, Shanghai University, Jiading, Shanghai 201800, People's Republic of China.

[b] Key Laboratory of Advanced Display and System Applications, Ministry of Education, Shanghai University, Shanghai 200072, People's Republic of China.

## Abstract:

We have fabricated novel BaZnSnO-TFT using solution process and investigated the electrical performance and temperature stability. BaZnSnO-TFT shows an improved field-effect mobility of 3.2 $cm^2/V$ s, a subthreshold swing of 0.61 V/decade and an on/off current ratio of $2\times10^7$ compared to those of ZnSnO-TFT. Density of state distribution of BaZnSnO and ZnSnO semiconductor has been extracted from electrical measurements. BaZnSnO-TFT shows an improved electrical performance and temperature stability due to smaller oxygen vacancies, less bulk trap density and interface state density.

## Keywords:

BaZnSnO-TFT, temperature stress, solution process

[*] Corresponding author: E-mail address: lijun_yt@163.com (J. Li), jhzhang@staff.shu.edu.cn (J. H. Zhang)



RSC Advances Accepted Manuscript

RSC Advances Accepted Manuscript

## 1. Introduction

Recently, thin film transistors (TFTs) based on oxide semiconductor have been reported as an alternative of amorphous silicon (a-Si) TFTs due to high mobility, high stability and transparency in visible light region [1, 2]. Many deposition methods such as radio frequency magnetron sputtering, pulse laser deposition, and solution process, were reported to prepare oxide thin film. Solution-processed oxide thin films as a channel layer of TFTs are paid more attention due to simple, low cost, large area uniformity and various compositions of oxide thin films.

For realization of high performance of oxide TFTs, In-based semiconductors such as InZnO, InGaZnO, and HfInZnO, have been frequently reported [3, 4]. $In^{3+}$ is favorable to achieve high mobility due to its special electron configuration of $4d^{10}5s^{0}$ [5]. However, a rare-earth indium element is expensive, toxic, and unstable in hydrogen plasma, which will enhance the fabrication cost of transistor. Sn-based oxide semiconductor has become a competitive alternative for indium because $Sn^{4+}$ has a similar electron configuration with $In^{3+}$ and amorphous ZnSnO-TFTs have achieved high performances comparable with InGaZnO-TFTs. In order to reduce oxygen vacancies of ZnSnO film, Si, Zr, Al element have been doped into ZnSnO film to suppress oxygen vacancies [6-8]. To find more effective carrier suppressors, we have considered three important factors consisting of low standard electrode potential (SEP), larger bandgap, and low electro-negativity. For this reason, Ba is also an attractive material for carrier suppressors due to its low SEP (-2.90 V), wide bandgap (4.8 eV) and lower electro-negativity (0.89). Here, solution-processed BaZnSnO film

as an active layer of TFTs was firstly reported.

The field effect mobility of oxide TFTs is acceptable for next-generation flat panel displays. Thin film transistors are affected by ambient temperature and self-heating in the work process. Thus, the device reliability including temperature instability has already limited the development of oxide TFTs into commercial electron electronic products. For commercial application, precise knowledge of the mechanism of temperature instability is necessary. Density of states (DOS) including the interfacial trap density and bulk trap density has a strong influence on temperature instability. In this work, we have fabricated a novel BaZnSnO-TFT and firstly studied the temperature instability. DOS distribution of BaZnSnO semiconductor has been extracted from electrical measurements. It provides a quantitative analysis that correlates the temperature instability of BaZnSnO-TFT to DOS parameters.

## 2. Experimental details

BaZnSnO thin film was prepared using zinc acetate dehydrate ($Zn(CH_3COO)_2 \cdot 2H_2O$ ), tin chloride dehydrate ($SnCl_2 \cdot 2H_2O$) and barium nitrate ($Ba(NO_3)_2$). These precursors were dissolved in 2-methoxyethanol. A 0.1 M monoethanolamine (MEA) was then added in the precursor solution as a sol-gel stabilizer. The concentration of metal precursors was 0.25 M and the molar ratio was 1:2: 0.15 for Zn: Sn: Ba. The solution was stirred at 50 ℃ for 3 h.

A bottom-gate-type TFT was fabricated. Highly doped n-type silicon wafer with 0.01-0.025 Ω cm was used as substrate and gate electrode. A 300-nm thick $SiO_2$ used as a gate dielectric was fabricated by thermal oxidation on the high-doped n-type



RSC Advances Accepted Manuscript

RSC Advances Accepted Manuscript

silicon wafer. Prior to processing, the wafer was cleaned with a standard wet-cleaning procedure. The BaZnSnO film were prepared by spin-coating at 3000 rpm for 30 s and prebaked at 200 ℃ for 20 min. Subsequently, the wafer was annealed at 500 ℃ for 80 min in ambient air. Finally, a 60-nm-thick Al film was sequentially vacuum deposited onto active layer using a metal mask to define transistor with channel width $W$=1000 μm and channel length $L$=200 μm.

The current–voltage characteristics of the devices were measured using an Agilent 4155C semiconductor analyzer. The capacitance measurements were conducted with an Agilent E4980A Precision LCR meter. The thickness of thin film was determined by a surface profiler (Alpha-Step IQ). X-ray diffraction (XRD) scans were measured with a Rigaku D\Max-2200 X-ray diffractometer using Cu Kα radiation. Optical properties of thin films were measured using a UV-vis spectrophotometer. The chemical bonding states of films was carried out with the x-ray photoelectron spectroscopy (XPS) (Thermo-ESCALAB 250Xl). All measurements were carried out at room temperature.

## 3. Results and discussion

Fig. 1 (a) shows the X-ray diffraction pattern of the ZnSnO and BaZnSnO(0.15) film prepared on $SiO_2$/Si substrate and annealed at 500 ℃ for 80 min. The ZnSnO film and BaZnSnO film show amorphous phase with no prominent peak. The amorphous oxide thin films have more uniform structures and smoother surfaces which could yield smooth channel /gate insulator interface. The optical transmittance spectra of ZnSnO and BaZnSnO(0.15) film on the glass substrate were characterized

as shown in Fig. 1(b). The average transmittances in the range of 400-700 nm are over 87 % for both films. The energy bandgap ($E_g$) can be obtained by using the following equation:

$$(\alpha h\gamma)^2 = \beta(h\gamma - E_g) \qquad (1)$$

Where $h$ is Planck's constant, $\gamma$ is the frequency of incident photon, and $\beta$ is energy independent constant. $E$g can be obtained by extrapolating the linear portion of the $(\alpha h\gamma)^2$ and hγ plots to the energy axis, as shown in the inset of Fig. 1(b). The band gap of BaZnSnO(0.15) film is obtained to be 3.51 eV. The bandgap of undoped ZnSnO film is 3.40 eV. The broadening of band gap of BaZnSnO leads to a reduction in the electron charge carrier and an increase in the activation energy. On the other hand, the broadening of band gap of BaZnSnO film makes the climb of carrier from the valence band to the conduction band more difficult [9, 10].

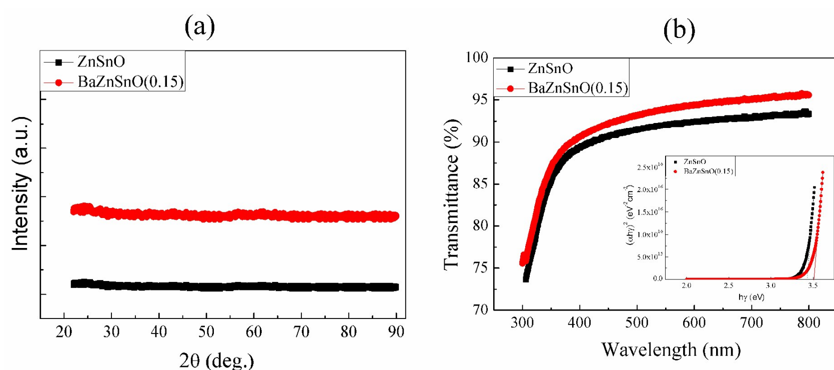


Fig. 1 (a) The X-ray diffraction pattern of the ZnSnO and BaZnSnO(0.15) film. (b) The optical transmittance spectra of ZnSnO and BaZnSnO(0.15) film on the glass substrate.



RSC Advances Accepted Manuscript

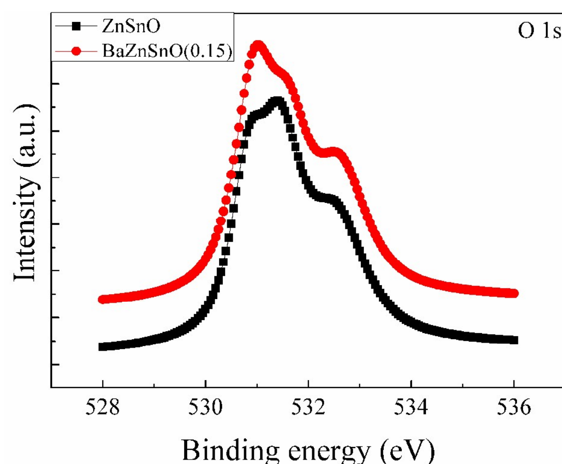


Fig. 2. O1s peaks of XPS spectra of ZnSnO and BaZnSnO film.

Fig. 2 shows O1s peaks of XPS spectra of ZnSnO and BaZnSnO(0.15) film. The O1s region of the XPS spectrum can be divided into three regions: low binding energy ($O_{I}$, 530.7 eV), media binding energy ($O_{II}$, 531.5 eV) and high binding energy ($O_{III}$, 532.5 eV). The $O_{I}$ peak indicates a metal-oxygen lattice peak without oxygen deficiency. Similarly, the $O_{II}$ and $O_{III}$ are related to the $O^{2-}$ ions located in the oxygen deficient region in the film and bonded oxygen such as $H_2O$, $O_2$ on the film surface or inside thin films, respectively. The change of Vo concentration can be depicted by the peak area variation of $O_{II}$ component. The integral areas of $O_{I}$, $O_{II}$ and $O_{III}$ can be obtained by fitting the XPS spectra of O1s. $S_1$, $S_2$, and $S_3$ represent the integral areas of $O_{I}$, $O_{II}$ and $O_{III}$ peak, respectively. $S_{tot}$ is the sum of the integral areas of $O_{I}$, $O_{II}$ and $O_{III}$ peak. Interestingly, $S_2/S_{tot}$ value of BaZnSnO film is about 25.9 %, which is smaller than that of the ZnSnO film (34.2%). It indicates that Ba acted as a carrier suppressor in the ZnSnO film. Ba ions are easily to form stronger chemical bonds with oxygen than Zn and Sn ions, which can attributed to the relatively high bond strength of Ba-O (562 KJ/mol) comparing with Zn-O (395 KJ/mol) and Sn-O (531.8



RSC Advances Accepted Manuscript

KJ/mol). Thus, Ba can effectively suppress the formation of oxygen vacancies and lower oxygen vacancies are favorable to improve stability of thin film transistor.

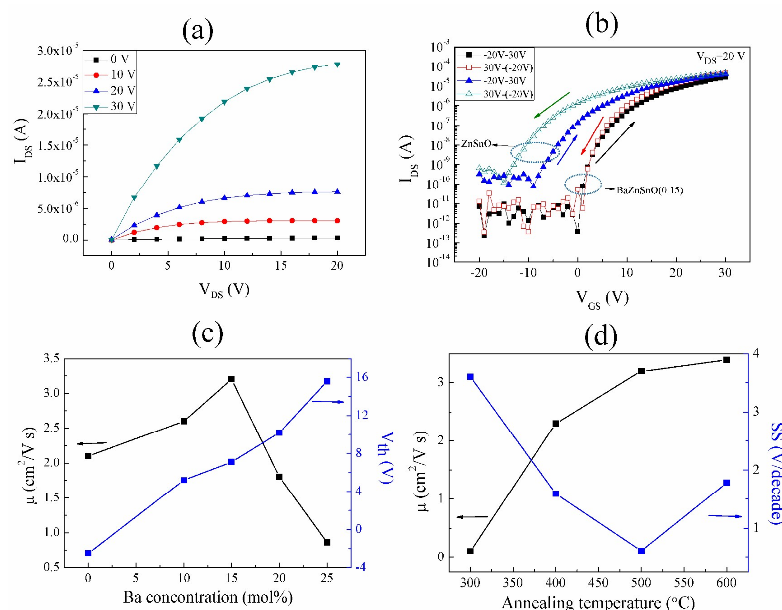


Fig. 3.The (a) output and (b) the electrical hysteresis of the BaZnSnO(0.15)-TFT tested at room temperature. the effect of (c) Ba ratio and (d) annealing temperature on the electrical performance of BaZnSnO-TFT.

Fig. 3(a) and (b) shows the output characteristics of the BaZnSnO(0.15)-TFT tested at room temperature, respectively. The BaZnSnO-TFT shows a normally off type n-channel enhanced-mode behavior. No current crowding is observed from Fig. 3(a) indicating good ohmic contacts between BaZnSnO channel layer and Al source/drain electrode. Fig. 3(b) shows the electrical hysteresis of source-to-drain current ($I_{DS}$) as a function of $V_{GS}$ with the fixed drain voltage ($V_{DS}$) at 20 V for BaZnSnO(0.15)-TFT. The $V_{GS}$ is swept by 1 V increments along a forward sweep from -20 V to 30V and along a reverse sweep from 30 V to -20 V. The clockwise hysteresis suggests that negative charge carriers are trapped at the interface between the channel and the gate



RSC Advances Accepted Manuscript

insulator or injected into the gate insulator from the channel [11]. The electrical hysteresis of BaZnSnO(0.15)-TFT is obviously better than that of ZnSnO-TFT. The results clearly indicate the poor stability of ZnSnO-TFTs, which could be attributed to charge trapping at the bulk and the $ZnSnO/SiO_2$ interface. BaZnSnO(0.15)-TFT shows no obvious hysteresis, indicating that less negative charge carriers are trapped at the interface between the channel and the gate insulator or injected into the gate insulator. The result is also verified by the smaller subthreshold swing. The mobility of the BaZnSnO-TFT in the saturation region was extracted from the following equation:

$$I_{DS} = \frac{W}{2L}\mu C_i\left[(V_{GS} - V_{th})^2\right] \qquad (1)$$

Where $I_{DS}$ is the drain-source current, $W$ is the width of channel, $L$ is the length of channel, $C_\mathrm{i}$ is the capacitance per unit area of the insulator layer ($C_i$=10.0 nF/cm$^2$), $V_\mathrm{GS}$ is the gate voltage, $\mu$ is the saturation mobility and $V_\mathrm{th}$ is the threshold voltage. The $V_{th}$ of the devices was determined by extrapolating the $I_{DS}^{1/2}$ vs. $V_{GS}$ plot to $I_{DS}$=0. In addition, the subthreshold swing ($SS$) is calculated from the subthreshold region using the following equation

$$SS = \frac{dV_{GS}}{d(\log I_{DS})} \qquad (2)$$

$SS$ is given by the maximum slope in the transfer curve. The BaZnSnO-TFT shows a $\mu$, $V_\mathrm{th}$, $I_\mathrm{on/off}$, and $SS$ of 3.2 cm$^2$/V s, 7.1 V, $2\times10^7$, and 0.61 V/decade, respectively. In addition, the maximum interfacial traps density ($N_\mathrm{it}$) can be estimated from the following equation:



RSC Advances Accepted Manuscript

$$N_{it} = \left[ \frac{SS\log(e)}{KT/q} - 1 \right] \frac{C_i}{q} \qquad (3)$$

where $k$ is Boltzmann constant, $q$ is the elementary electron charge and $T$ is the absolution temperature. The $N_{it,max}$ value of BaZnSnO-TFT is estimated to be $5.7\times 10^{11}$ $cm^{-2}$, which is comparable with the published value for sputtered InGaZnO-TFT fabricated on a $SiO_2$-based substrate [12, 13]. The low $N_{it}$ means that BaZnSnO-TFT has a low charge trapping at the BaZnSnO/$SiO_2$ interface. For comparison, ZnSnO-TFT is fabricated and electrical performance is investigated, as shown in Fig. 3(b).

The effect of Ba ratio and annealing temperature on the electrical performance of BaZnSnO-TFT is investigated. The electrical performance of BaZnSnO-TFT at a $V_{DS}$ of 20 V for various Ba content levels is shown in Fig. 3(c). The 15 mol% Ba-doped ZnSnO-TFT has the highest saturation mobility value of 3.2 $cm^2$/V s. When the Ba content is 25 mol%, the saturation mobility decreases from 3.2 to 0.86 $cm^2$/V s. As the Ba content increases, the threshold voltage increases monotonically from -2.5 to 15.6 V. The result is attributed to the excess Ba addition results in the lower carrier concentration and the decreased conductivity of the channel layer. The saturation mobility and the subthreshold swing as a function of the annealing temperature are shown in Fig. 3(d). when the annealing temperature is increased to 300 to 600 ℃, the saturation mobility increases from 0.2 to 3.4 $cm^2$/V s. The result is due to the increase in the number of native defects especially oxygen vacancies with the annealing temperature increasing. Unfortunately, the excess oxygen deficiencies induced by high temperature will lead to a high $SS$ value. It is easily seen that BaZnSnO(0.15)-TFT shows a superior electrical performance. BaZnSnO(0.15)-TFT



RSC Advances Accepted Manuscript

shows an improved field-effect mobility of 3.2 $cm^2$/V s, a subthreshold swing of 0.61 V/decade and an on/off current ratio of $2\times10^7$. It is concluded that Ba doping can suppress oxygen vacancies and reduce the interface trap state, and thus improve the device characteristics. In short, the BaZnSnO(0.15)-TFT exhibits an acceptable electrical performance for next-generation flat panel displays.

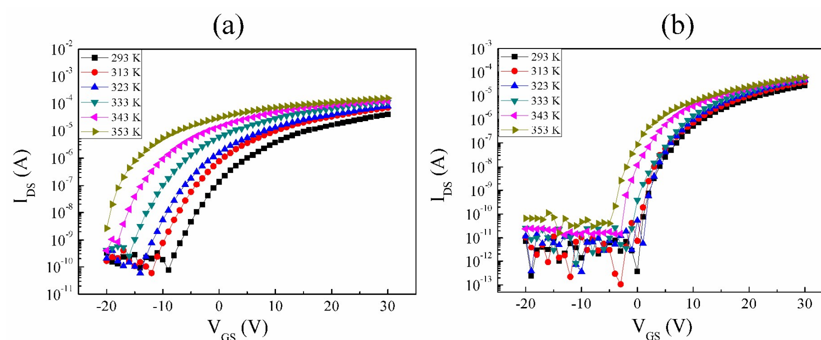


Fig.4. The evolution of the transfer characteristic of ZnSnO-TFT and BaZnSnO(0.15)-TFT as a function of the temperature.

Fig. 4 shows the evolution of the transfer characteristic of ZnSnO-TFT and BaZnSnO-TFT as a function of the temperature. For both devices, the transfer curves are negatively shifted with increasing temperature. As the temperature increases from 293 K to 353 K, $V_{th}$ of ZnSnO-TFT is shifted by approximately -13.6 V from -2.5 to -16.1 V. However, the corresponding negative $V_{th}$ shift in BaZnSnO-TFT is relatively small. $V_{th}$ of BaZnSnO-TFT is shifted by approximately -4.7 V from 7.1 to 2.4 V for BaZnSnO-TFT. BaZnSnO-TFT shows a smaller $V_{th}$ shift than that of ZnSnO-TFT. At higher temperatures, more electrons can escape from the localized states and contribute to the free carriers, which cause a smaller threshold voltage. The negative $V_{th}$ shift with increasing temperature may be related to the shift of the Femi level $E_F$.

RSC Advances Accepted Manuscript

The shift of $E_F$ can be expressed by the variation of the conduction activation energy ($E_a$). $E_a$ is the energy difference between $E_F$ and the edge of the conduction band ($E_C$), which equates to the average energy that a trapped electron escapes from the localized state. In case of general thin film transistors, the temperature dependence of the $V_{th}$ shift is closely related with the increase in thermally active electrons. It is necessary to investigate the impact of thermally activated process on the change in free electrons. In generally, the generated free electrons in oxide semiconductors are mainly attributed to oxygen vacancies [14]. It is reported that thermally activated electrons are exponentially increased with increasing temperature [15]. The drain current ($I_{DS}$) is thermally activated and can be described by [16, 17]:

$$I_{DS} = I_{DS0} \cdot \exp(-E_a / kT) \qquad (4)$$

where $I_{DS0}$ is the prefactor, $k$ is the Boltzmann constant, $T$ is the temperature, $E_a$ can be estimated by fitting of temperature-dependent log ($I_{DS}$) versus 1/$T$ curve as shown in Fig. 5. It is assumed that thermally activated electron from deep level trap sites into the conduction band move quickly toward the drain electrode under a electrical field. Thus, the rate-limiting process would involve thermal excitation of the trapped charge, and $E_a$ can be extracted as a function of $V_{GS}$ in the forbidden bandgap (as shown in Fig. 6(a)). The maximum $E_a$ value is obtained to be 1.14 eV at a $V_{GS}$ of -12 V. For BaZnSnO-TFT, the maximum $E_a$ value is about 1.09 eV at a $V_{GS}$ of 0 V, which is similar with the reported value by H. Godo et al [18]. $E$a value decreases with increasing $V_{GS}$. The decreasing rate of $E$a are estimated to be 0.23 eV/V for BaZnSnO-TFT and 0.11 eV/V for ZnSnO-TFT, indicating that BaZnSnO



RSC Advances Accepted Manuscript

semiconductor shows a fast moving $E_F$ level of with respective to $V_{GS}$. The rate of change in $E_F$ level of with respective to $V_{GS}$ is inversely proportional to the magnitude of total trap density ($N_{tot}$) including the density of state (DOS) of bulk semiconductor film and interface trap density between active layer and $SiO_2$ film. The result suggests that BaZnSnO-TFT exhibits a relatively low bulk and interface trap density.

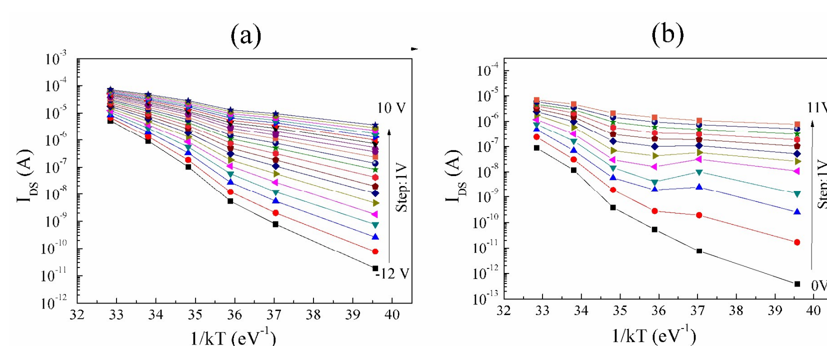


Fig. 5. Relationship between log ($I_{DS}$) and $1/T$ as a function of $V_{GS}$ for (a) ZnSnO-TFT and (b)BaZnSnO(0.15)-TFT.

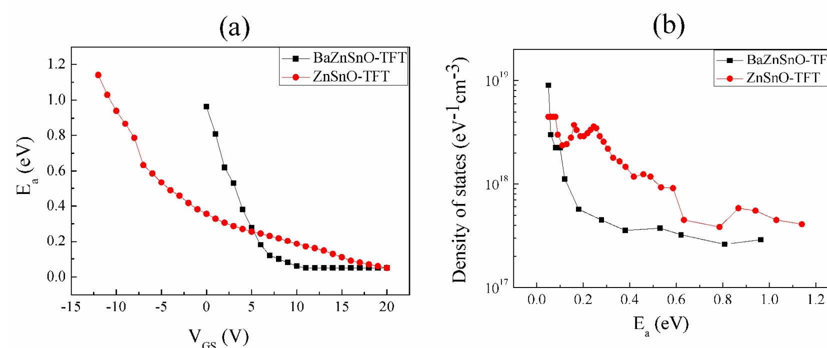


Fig. 6. (a) The relation between $V_{GS}$ and $E_a$. (b) calculated DOS distribution as a function of $E_a$.

The density of states (DOS) of the BaZnSnO-TFT and ZnSnO-TFT can be



RSC Advances Accepted Manuscript

extracted from the relationship between $E_a$ and $V_{GS}$ by assuming the current in the active layer distributed uniformly in several hundred angstroms of active layer. The DOS can be calculated using the following equation [19].

$$g(E_a) = -\frac{\varepsilon_i}{qd_i t \frac{d(E_a)}{d(V_{GS})}} \qquad (5)$$

Where $\varepsilon_i$ and $d_i$ are respectively the permittivity and the thickness of the gate dielectric, $t$ is the thickness of the active layer, and $q$ is the electron charge. Fig. 6 (b) shows the relationship between density of state and activation energy of BaZnSnO-TFT and ZnSnO-TFT. For BaZnSnO-TFT, the magnitude of density decreases from $8.9\times10^{18}$ to $2.8\times10^{17}$ $cm^{-3}$ as the activation energy increases. The calculated DOS distribution is comparable to the reported solution-processed HfInZnO-TFT [20]. The total DOS for BaZnSnO-TFT is obviously smaller than that for ZnSnO-TFT at a specific energy level. The total DOS value at a specific energy level is the summation of bulk trap density and interface state density. Compared with ZnSnO-TFT, BaZnSnO TFTs have a lower density of trap states in the subgap DOS, which leads to superior electrical performance and better temperature stability. Thus, BaZnSnO film could be a useful active layer for high performance thin film transistors.

## 4. Conclusions

In summary, we have fabricated BaZnSnO-TFT by solution process. Compared to the ZnSnO-TFT, BaZnSnO(0.15)-TFT exhibits a better electrical performance and temperature stability. Extraction of the DOS of transistor using temperature-dependent



RSC Advances Accepted Manuscript

field effect measurement is used to understand the electrical performance and stability. It is attributed that much smaller oxygen vacancies and DOS distribution compared to the ZnSnO-TFT.

## 5. Acknowledgements

The authors would like to acknowledge the financial support given by the Natural Science Foundation of China (51302165, 61274082, 61077013), Shanghai Municipal Education Commission (ZZSD13047), Innovation Fund of shanghai University and China Postdoctoral Science Special Fund (2012T50387).

## References

[1] K. Nomura, H. Ohta, K. Ueda, T. Kamiya, M. Hirano, H. Hosono, Science 300 (2003) 1269.

[2] H. J. Kwang, J. I. Kim, H. Y. Jung, S. Y. Park, R. Choi, K. K. Un, S. H. Cheol, D. Lee, H. Hwang, J. K. Jeong, Appl. Phys. Lett. 10 (2011) 101101.

[3] B. D. Ahn, J. S. Park, K. B. Chung, Appl. Phys. Lett. 105 (2014) 163505.

[4] J. Li, J. H. Zhang, X. W. Ding, W. Q. Zhu, X. Y. Jiang, Z. L. Zhang, Thin Solid Films 562 (2014) 592.

[5] K. Nomura, H. Ohta, A. Takagi, T. Kamiya, M. Hirano, H. Hosono, Nature 432 (2004) 488.

[6] C. Wu, X. Li, J. Lu, Z. Ye, J. Zhang, T. Zhou, R. Sun, L. Chen, B. Lu, X. Pan, Appl. Phys. Lett. 103 (2013) 082109.

[7] P. T. Tue, T. Miyasako, J. Li, H. T. C. Tu, S. Inoue, E. Tokumitsu, T. Shimoda, IEEE Trans. Electron Devices 60 (2013) 320.

[8] H. J. Jeon, W. J. Maeng, J. S. Park, Ceram. Int. 40 (2014) 8769.

[9] G. H. Kim, W. H. Jeong, B. D. Ahn, H. S. Shin, H. J. Kim, H. J. Kim, M. K. Ryu,

RSC Advances Accepted Manuscript

K. B. Park, J. B. Seon, S. Y. Lee, Appl. Phys. Lett. 96 (2010) 163506.

[10] B. Y. Su, S. Y. Chu, Y. D. Juang, S. Y. Liu, J. Alloy. Compd. 580 (2013) 10.

[11] T. Jun, K. Song, Y. Jeong, K. Woo, D. Kim, C. Bae, J. Moon, J. Mater. Chem. 21 (2011) 1102.

[12] H. C. Wu, C. H. Chien, Appl. Phys. Lett. 102 (2013) 062103.

[13] J. Li, F. Zhou, H. P. Lin, W. Q. Zhu, J. H. Zhang, X. Y. Jiang, Z. L. Zhang, Vacuum 86 (2012) 1840.

[14] K. Hoshino, J. F. Wager, IEEE Electron Device Lett. 31 (2010) 818.

[15] K. Kim, P. C. Debnath, S. Kim, and S. Y. Lee, Appl. Phys. Lett. 98 (2011) 113109.

[16] C. Chen, K. Abe, H. Kumomi, and J. Kanicki, IEEE Trans. Electron Devices 56 (2009) 1177-1182.

[17]D. H. Kim, H. K. Jung, D. H. Kim, and S. Y. Lee, Appl. Phys. Lett. 99 (2011) 162101.

[18] H. Godo, D. Kawae, S. Yoshitomi, T. Sasaki, S. Ito, H. Ohara, H. Kishida, M. Takahashi, A. Miyanaga, S. Yamazaki, Jpn. J. Appl. Phys. 49 (2010) 03CB04.

[19] Y. H. Tai, H. L. Chiu, L .S. Chou, J. Electrochem. Soc. 159 (2012) J200.

[20] W. H. Jeong, G. H. Kim, H. S. Shin, B. D. Ahn, H. J. Kim, M. K. Ryu, K. B. Park, J. B. Seon, S. Y. Lee, Appl. Phys. Lett. 96 (2010) 093503.

RSC Advances Accepted Manuscript